Spatial-Temporal Current Source Correlations and Cortical Connectivity

R. W. Thatcher, C. J. Biver and D. North

Key Words

Cortical Connections
Cortico-cortical Connectivity Model
Intra-hemispheric Asymmetry
LORETA
Source Correlations

ABSTRACT

The purpose of this study was to explore spatial-temporal correlations between 3-dimensional current density estimates using Low Resolution Electromagnetic Tomography (LORETA).

The electroencephalogram (EEG) was recorded from 19 scalp locations from 97 subjects. LORETA current density was computed for 2,394 gray matter pixels. The gray matter pixels were grouped into 33 left hemisphere and 33 right hemisphere regions of interest (ROIs) based on groupings of Brodmann areas. The average source current density in a given region of interest (ROI) was computed for each 2 second epoch of EEG and then a Pearson product correlation coefficient was computed over the time series of successive 2 second epochs of current density between all pairwise combinations of ROIs during the resting eyes-closed EEG session.

Rhythmic changes in source correlation as a function of distance were present in all regions of interest. Also, maximum correlations at certain frequencies were present independent of distance. The occipital regions exhibited the highest short distance correlations and the frontal regions exhibited the highest long distance correlations. In general, the right hemisphere exhibited higher intra-hemispheric source correlations than the left hemisphere especially in the temporal, parietal and occipital cortex. The strongest left vs. right hemisphere differences were in the alpha frequency band (8-12 Hz) and in the gamma frequency band (37-40 Hz).

The pattern of spatial frequencies in different cortical lobules is consistent with differences in neural packing density and the operation of 'U' shaped fiber systems. The general conclusions were: 1- the higher the packing density then the greater the intra-cortical connection contribution to LORETA source correlations, 2- spatial frequencies are primarily due to intra-cortical 'U' shaped fiber connections and long distance fiber connections, 3- posterior and temporal cortical intra-hemispheric coupling is generally stronger in the right hemisphere than in the left hemisphere.

INTRODUCTION

Neural dynamics involves the generation of electrical currents by populations of synchronously active neurons within local regions of the brain which are coupled through axonal connections to other populations of neurons.[1-4] Anatomical analyses of the cerebral white matter have shown that there are three general categories of cortico-cortcal connections: 1- intra-cortical unmyelinated connections within the gray matter on the order of 1 mm to approximately 3 mm, 2- short-distance 'U' shaped fibers in the cerebral white matter located beneath the gray matter (10 mm to approx. 30 mm) and, 3- long distance fasciculi located in the deep white matter below the 'U' shaped fibers with distances from 30 mm to approx. 170 mm.[3,4] Measures of EEG coherence and phase delays from the scalp surface commonly detect the presence of two compartments with an approximate correspondence with the short distance and long distance fiber systems.[1,2,5-7] For example, studies by Nunez[1] and Thatcher et al[5] showed that EEG coherence decreases as a function of distance from any electrode site, thus characterizing the short distance compartment and coherence increases as a function of distance beyond approximately 10-14 cm, which characterizes the long distance compartment. Studies of changes of EEG coherence with distance are usually explained by a decrease in the number of connections as a function of distance from any given population of neurons, while increased coherence with distance is explained by an increase of connections between two populations through axons and fasciculi of the deep cerebral white matter.[1-6]

A deeper understanding of cortical coupling is possible by studying the correlations between current sources derived from the surface EEG using an inverse method.[8-10] Thatcher et al[8] recorded EEG during voluntary finger move-
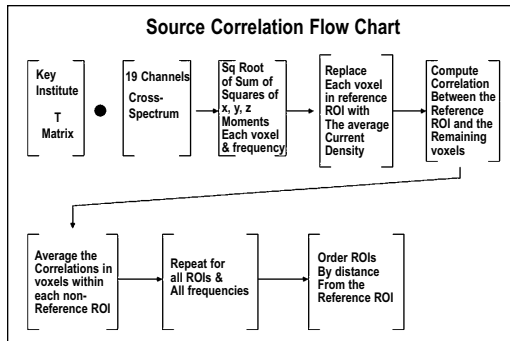
Figure 1.

Flow chart of the procedures to compute LORETA source correlations.

ments and derived three dipoles in the sensory-motor cortical regions that accounted for approximately 97% of the variance of the surface EEG and were validated using PET and MRI. A pseudo-inverse procedure was then used to derive three different time series from each of the three dipoles, and coherence and phase delays were computed between the various combinations of dipole time series. Stable but rapid changes in correlations between sources were shown to be time locked to voluntary motor movements in the supplemental motor cortex and the contra-lateral motor cortex.[8,9] Hoechstetter et al[10] used a multiple dipole source solution for scalp EEG electrical potentials and then used coherence to compute the correlation between the 3-dimensional current sources and demonstrated changes in the correlation between current sources related to different tasks. Pascual-Marqui et al[11] used low resolution electromagnetic tomography (LORETA) to compute current sources and then used a correlation coefficient to explore differences in source correlations between a normal control group and a group of schizophrenic patients. All of these studies revealed interesting and reproducible relations between current sources and network connectivity that provide a deeper understanding of the surface EEG dynamics.

A general limitation of all LORETA studies is the use of a "Low Resolution" point spread function by the Laplacian operator when using 19 scalp electrodes.[12] For example, the spatial correlation of magnitudes is approximately unity between nearby voxels and decreases as a smooth and monotonic function of distance. However, the point spread function is not a major difficulty when spatial correlations are computed over intervals of time, because the null hypothesis is that spatial frequency is constant over time and approximates a monotonic function. Significant deviations from a monotonic function of distance are independent of the effects of a point-spread and therefore must be explained by other factors such as the anatomical location of spatio-temporally associated ROIs. A method employed in this study is to minimize the effects of point spread by clustering groups of nearby voxels as "Regions of Interest" (ROIs) and then

compute the time covariance of current density magnitudes. The point-spread is constant over time, and thus spatial frequencies of correlations can not be explained by a simple point-spread model of any EEG inverse solution.

The purpose of the present paper is to evaluate the use of low resolution electromagnetic tomography (LORETA) to compute the spatio-temporal correlation coefficient or temporal covariance of current source density between regions of interest as defined by Brodmann areas. Specific experimental hypotheses are: 1- source correlations decrease smoothly as a function of distance from a given region of interest (point-spread null hypothesis), 2- source correlations are isomorphic or uniform as a function of frequency (uniform resonance null hypothesis) and , 3- there are no differences in intra-hemispheric source correlations between homologous left and right hemisphere locations (hemispheric null hypothesis).

METHODS
Subjects

A total of 97 normal adults ranging in age from 5 to 37 (male = 58, mean age = 10.41 years, standard deviation of age = 4.66) were included in this study. The subjects in the study were selected based on no history of neurological disorders such as epilepsy, head injuries and reported normal development and successful school performance. A Wechsler Intelligence test was administered to all subjects and the range of full scale I.Q. was 120 to 154. The age range and gender proportion is the result of including all subjects that met the no clinical disorder criteria and with I.Q. scores > 120.

EEG recording

The EEG was recorded from 19 scalp locations based on the International 10/20 System of electrode placement, using linked ears as a reference. Each EEG record was plotted and visually examined and then edited to remove artifact. The amplifier bandwidths were nominally 0.5 to 40 Hz, the outputs being 3 db down at these frequencies, and the sample rate was 128 Hz. Split-half and test-re-test reliability measures were conducted on the edited EEG segments and only records with > 95% reliability were entered into the spectral analyses. EEG was acquired in the eyes-closed conditions and record lengths varied from 58.6 seconds to 120 seconds.

Cross-spectral analysis and LORETA computation

The temporal covariance or correlation of LORETA current density between successive 2 second FFT epochs over the 58 second to 120 seconds is the subject of this study. The steps to compute the desired spatial-temporal correlations between regions of interest are described in Figure 1. First step is the digitized EEG samples divided into successive 2 second epochs of 256 sample points of the edited EEG then FFT cross-spectral analysis using a cosine taper window according to standard procedures for LORETA frequency analyses.[13-15] In

Table 1					
Examples of spatial ordering of ROIs for the superior frontal gyrus and the middle occipital gyrus					
Superior Frontal Gyrus			Middle Occipital Gyrus		
	Region	(mm)		Region	(mm)
MFG	Medial Frontal Gyrus	17.63	IOG	Inferior Occipital Gyrus	13.96
MidFG	Middle Frontal Gyrus	20.82	SOG	Superior Occipital Gyrus	20.47
AC	Anterior Cingulate	26.24	AG	Angular Gyrus	29.91
IFG	Inferior Frontal Gyrus	40.21	LG	Lingual Gyrus	30.03
EN	Extra-Nuclear	48.66	Cu	Cuneus	31.64
PreCG	Precentral Gyrus	52.96	PC	Posterior Cingulate	38.38
SG	Subcallosal Gyrus	51.08	SMG	Supramarginal Gyrus	43.02
CG	Cingulate Gyrus	53.33	FG	Fusiform Gyrus	44.56
OG	Orbital Gyrus	51.68	PCu	Precuneus	45.84
RG	Rectal Gyrus	52.77	MTG	Middle Temporal Gyrus	48.94
In	Insula	55.48	IPL	Inferior Parietal Lobule	50.95
SubG	Sub-Gyral	70.97	SPL	Superior Parietal Lobule	52.28
TTG	Transverse Temporal Gyrus	70.06	SubG	Sub-Gyral	58.55
PCG	Postcentral Gyrus	72.97	PHG	Parahippocampal Gyrus	59.42
STG	Superior Temporal Gyrus	71.42	ITG	Inferior Temporal Gyrus	60.37
Un	Uncus	72.51	PCG	Postcentral Gyrus	63.26
PCL	Paracentral Lobule	76.40	STG	Superior Temporal Gyrus	63.46
PHG	Parahippocampal Gyrus	76.13	TTG	Transverse Temporal Gyrus	67.00
IPL	Inferior Parietal Lobule	88.27	In	Insula	72.50
MTG	Middle Temporal Gyrus	87.54	PCL	Paracentral Lobule	74.46
ITG	Inferior Temporal Gyrus	89.62	CG	Cingulate Gyrus	80.05
SMG	Supramarginal Gyrus	95.80	PreCG	Precentral Gyrus	81.57
PC	Posterior Cingulate	96.81	Un	Uncus	83.70
FG	Fusiform Gyrus	96.36	EN	Extra-Nuclear	91.62
SPL	Superior Parietal Lobule	102.72	SG	Subcallosal Gyrus	93.98
PCu	Precuneus	104.04	IFG	Inferior Frontal Gyrus	103.83
AG	Angular Gyrus	108.61	MidFG	Middle Frontal Gyrus	111.36
LG	Lingual Gyrus	115.04	AC	Anterior Cingulate	114.05
Cu	Cuneus	119.81	MFG	Medial Frontal Gyrus	116.70
SOG	Superior Occipital Gyrus	122.93	RG	Rectal Gyrus	119.03
MOG	Middle Occipital Gyrus	122.70	SFG	Superior Frontal Gyrus	122.70
IOG	Inferior Occipital Gyrus	127.90	OG	Orbital Gyrus	133.22

order to reduce the number of variables, adjacent frequency 0.5 Hz bands were averaged to produce a 1 Hz resolution thus yielding a total of 40 frequency bands from 1 to 40 Hz. The Key Institute software was used to compute the T matrix according to the Talairach Atlas coordinates of the Montreal Neurological Institute's MRI average of 305 brains.[12-16] Based on the equations of the Key Institute[15] the diagonal elements (autospectrum) of the Hermitian cross-spectral matrix were multiplied by the T matrix at each 1 Hz frequency band for each 2 second epoch. The T matrix is a 3-dimensional matrix of x, y and z current source moments in each of the 2,394 gray matter pixels. The resultant current source vector at each voxel was computed as the square root of the sum of the squares for the x, y and z source moments for each 1 Hz frequency band.

Regions of interest (ROIs)

The anatomical names and Brodmann areas that correspond to each of the 2,394 gray matter pixels in Talairach Atlas coordinates was provided by Lancaster et al[16] as used by the Key Institute software, Pascual-Marqui.[15] The Key Institute's first best match to a given region of interest (ROI) was used for both Brodmann area values and anatomical names. After computing the LORETA source currents for each of the 2,394 gray matter pixels the Key-Talairach table of gray matter pixels was sorted by anatomical name and an average current source density for a given ROI was computed by summing the current values for each of the gray matter pixels in an ROI and then dividing by the number of pixels. This resulted in a total of 66 different averages of current source density for each 2 second epoch (33 ROIs from the left hemisphere and 33 ROIs

from the homologous right hemisphere). A second level of averaging involved averaging the current source densities in the four general Brodmann lobules of frontal, temporal, parietal and occipital, which yielded eight lobules of averaged current source density, four left and four right hemisphere lobules. An example of the spatial ordering and designations of regions of interest for the superior frontal gyrus and the middle occipital gyrus are shown in Table 1.

Source correlations

The current values within a selected ROI were averaged and each voxel in the selected ROI was replaced with the average value and the ROI with average current density values is called a "reference ROI." Then a Pearson Product correlation coefficient was computed between the reference ROI average current value and the current density values in the remainder of the 2,394 pixels as the covariance of magnitudes over the time series of 2 second epochs. The average correlation between a given reference ROI and a different ROI was computed by averaging the correlation coefficients between the reference ROI and the individual voxels that comprise a given ROI. This procedure was repeated for each of the 66 ROIs. The average correlation values range from -1 to +1, and the statistical significance level is determined by the number of degrees of freedom or the total number of 2 second epochs that span a given time series. For example, the time series degrees of freedom in this study ranged from 29 to 60 for the range of 58 seconds to 120 seconds EEG recordings.

Figure 1 is a diagrammatic illustration of the computational methods used to compute the Pearson product source correlations over the time interval of the recording period. The computational steps are shown in separate blocks.

Distance metric of current source correlations

A Euclidean distance metric was computed for each region of interest in two steps. Step one computed a separate average of the x, y and z Talairach atlas coordinates of each voxel within a region of interest. Step two involved computing the square root of the sum of the squares of absolute distance between the average x, y and z coordinates of a reference ROI with respect to a different ROI. The computation of the absolute distance is the difference between the average X of a reference ROI (i.e., X_1) and the average X coordinate of a second ROI (i.e., X_2) and the same for the Y and Z coordinates. The difference between the x, y and z coordinates is then squared and the square root was computed on the sum of the squares as shown in equation 1.

$$\text{Eq. 1 - } D = \sqrt{(\bar{X}_1 - \bar{X}_2)^2 + (\bar{Y}_1 - \bar{Y}_2)^2 + (\bar{Z}_1 - \bar{Z}_2)^2}$$

Where the bar above x, y and z denotes the average x, y and z coordinate value for a given ROI, therefore, a center of mass coordinate value for each ROI.

The ROIs were then ordered as a function of Euclidean distance with respect to a given reference ROI. Examples of the spatial ordering of ROIs are shown in Table 1 for reference ROIs being the superior frontal gyrus and the middle occipital gyrus.

RESULTS

Spatial and temporal heterogeneity of source correlations

Figures 2 and 3 are examples of contour maps of source correlations from two different subjects for the left and right hemisphere frontal ROIs and left and right hemisphere occipital ROIs. Because of space limitations it was not possible to show contour maps of all 97 subjects. The two subjects selected are exemplars and typical of the source correlations found in all of the subjects. There was great consistency and similarity across subjects. These are examples of the general pattern of maximal source correlations at short distance distances (e.g., 13 mm to approx. 3 cm) in occipital regions and maximal source correlations at longer distances in frontal cortical regions (e.g., 3 cm to approx. 13 cm). It can be seen in Figures 2 and 3 that there are higher short distance correlations when using the occipital reference ROI than the frontal reference ROI. All of the subjects in this study exhibited horizontal bands and spatial frequencies or a pattern of increasing and decreasing correlations as a function of distance from the reference ROI.

In occipital regions, the frequency of maximal short distance source correlations was essentially uniform from 1 to approximately 40 Hz with longer distance high source correlations between 35 to 40 Hz. In contrast, frontal cortical regions exhibited more heterogeneity with maximal source correlations at different frequencies and at a variety of intra-hemispheric distances. All cortical regions tended to show higher correlations between 35 to 40 Hz than at lower frequencies.

Figure 4 shows increases and decreases as a function of distance with respect to the middle occipital gyrus (dashed lines) and middle temporal gyrus (solid lines) from the left hemisphere (left) and right hemisphere (right). In all subjects, the occipital regions exhibited maximum source correlations at short distances with a rhythmic decline in correlation as a function of distance. In contrast, the temporal regions showed maximal source correlations at long distances and a pronounced rhythmic pattern as a function of distance.

Hemispheric differences in source correlations

Figure 5, top left, shows average source correlations across all subjects (N = 97) from the left superior frontal gyrus, top right are the average source correlations from the homologous right superior frontal gyrus and in the middle are the results of t-tests between the source correlations in the left and right intra-hemispheric superior frontal gyrus. The z-axis is color scaled as shown by the color bar. The x-axis is frequency (Hz), and the y-axis are regions of interest that were ordered as a function of distance from the superior frontal gyrus. The ordered distances between the reference ROI (superior frontal gyrus) and the remain-
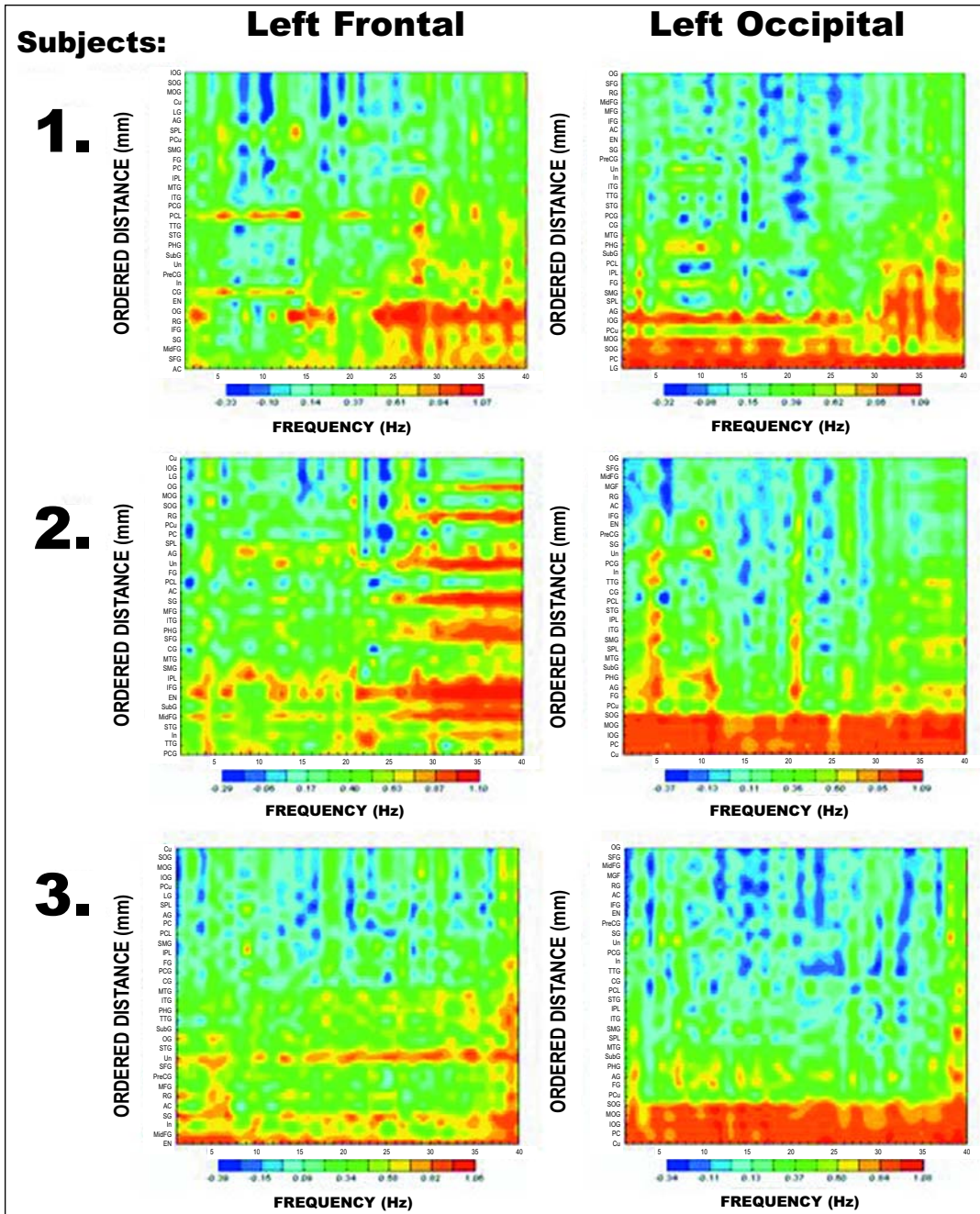
Figure 2.
Two-dimensional contour maps of the source correlations from two typical or examplar subjects from the left hemisphere superior frontal gyrus (left column) and the left hemisphere middle occipital gyrus (right column). The x-axis is frequency (1 to 40 Hz), the y-axis are ROIs that are ordered as a function of distance from the left superior frontal ROI (left column) and the left hemisphere middle occipital gyrus (right column). The z-axis is the magnitude of correlation as represented by the color bar under each contour map. The distances in the left column vary from 17.63 mm starting with the left hemisphere medial frontal gyrus that is the nearest ROI to the farthest distant ROI which is the left hemisphere inferior occipital gyrus (127.90 mm distant). The distances from the middle occipital gyrus in the right column vary from 13.96 mm for the left inferior occipital gyrus that is the nearest ROI to the most distant ROI which is the left hemi-sphere orbital frontal gyrus (132.22 mm distant). It can be seen that the occipital region exhibits shorter distance high source correlations than does the frontal region. See Table 1 for the names of the abbreviated ROIs and the distances from the reference ROI in millimeters.
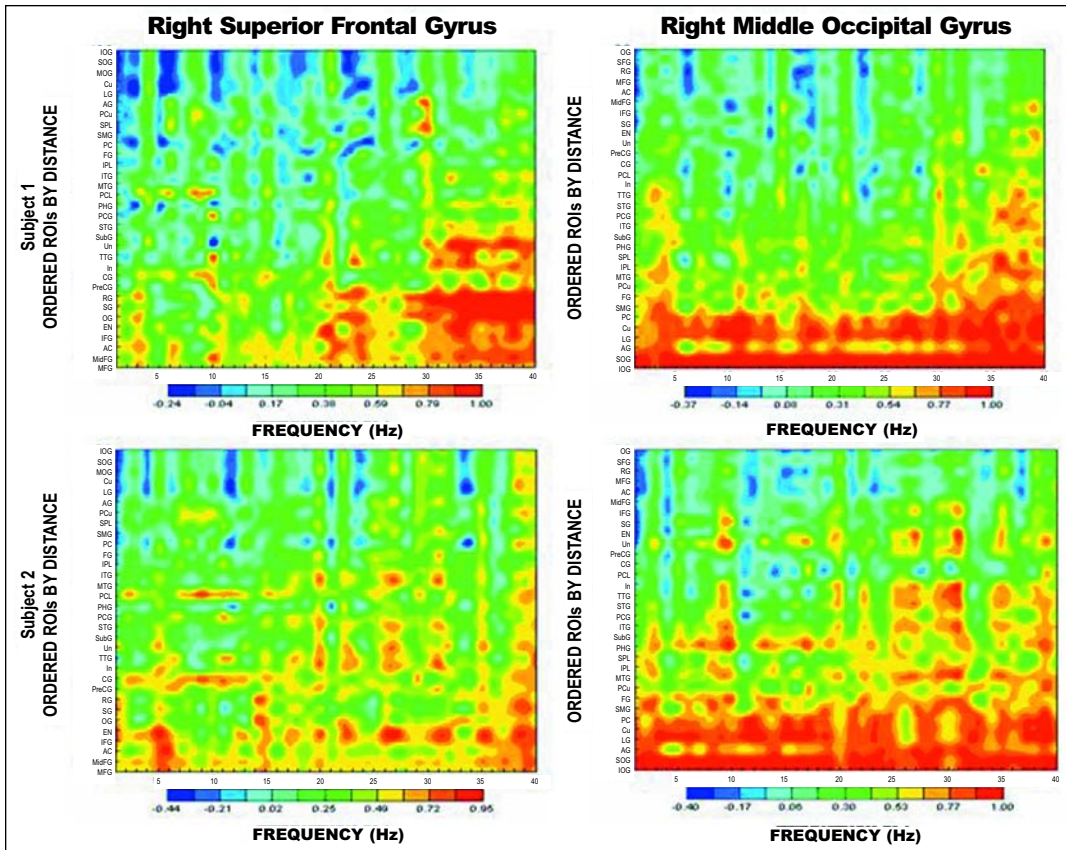
Figure 3.

Two-dimensional contour maps of the source correlations from the same two subjects as in Figure 2 but from the homologous right hemisphere superior frontal gyrus (left column) and the homologous right hemisphere middle occipital gyrus (right column). The x-axis is frequency (1 to 40 Hz), the y-axis are ROIs that are ordered as a function of distance from the superior frontal ROIt (left column) and the middle occipital gyrus (right column). The z-axis is the magnitude of correlation as represented by the color bar under each contour map. The distances in the left column vary from 17.63 mm starting with the right hemisphere medial frontal gyrus that is the nearest ROI to the farthest distant ROI which is the right hemisphere inferior occipital gyrus (127.90 mm distant). The distances from the middle occipital gyrus in the right column vary from 13.96 mm for the left inferior occipital gyrus that is the nearest ROI to the most distant ROI which is the left hemisphere orbital frontal gyrus (132.22 mm distant). It can be seen that the occipital region exhibits shorter distance high source correlations than does the frontal region. It can be seen that the right occipital region exhibits high source correlations at shorter distances than does the right hemisphere frontal region. See Table 1 for the names of the abbreviated ROIs. See Table 1 for the names of the abbreviated ROIs and the distances from the reference ROI in millimeters.

ing ROIs are shown in Table 1. T-test values less than P > .05 are colored green, while t-test differences where left intra-hemispheric source correlations are greater than the homologous right intra-hemispheric source correlations (positive) are colored orange to red. T-test differences where the right hemisphere source correlations were greater than the homologous left hemisphere source correlations (negative) are colored blue to purple. It can be seen that left superior frontal gyrus source correlations are significantly greater than right hemisphere source correlations (i.e., orange and red colors) especially at short distances and at frequencies greater than 20 Hz. The long distance source correlations (96 mm to 127 mm) are greater in the right superior frontal gyrus (i.e., blue and purple colors) than in the homologous left superior frontal gyrus, especially between 1 and 20 Hz.

Figure 6 top left are average source correlations (N = 97) from the left middle occipital gyrus, top right are the average source correlations from the homologous right middle occipital gyrus, and the middle are the results of t-tests between the source correlations in the left and right hemispheric middle occipital gyrus. The axes and color scaling are the same as in Figure 5. T-test values less than P > .05 are colored green while t-test differences where left hemisphere source correlations are greater than the homologous right hemisphere source correlations (posi-

Figure 4.
In the left column are mean source correlations from the left hemisphere middle temporal gyrus (solid line) and the left hemisphere middle occipital gyrus (dotted lines) at 9 Hz. In the right column are mean source correlations from the homologous right hemisphere middle temporal gyrus (solid line) and the right hemisphere middle occipital gyrus (dotted lines) at 9 Hz. The y-axis is mean source correlation and the x-axis is the ordered distance (millimeters) from the middle temporal and middle occipital gyri to the remaining ROIs. A linear decline in source

correlation is seen with occipital reference ROIs (dotted lines) where as there is a more complex spatial relationship with the temporal reference ROIs (solid line).
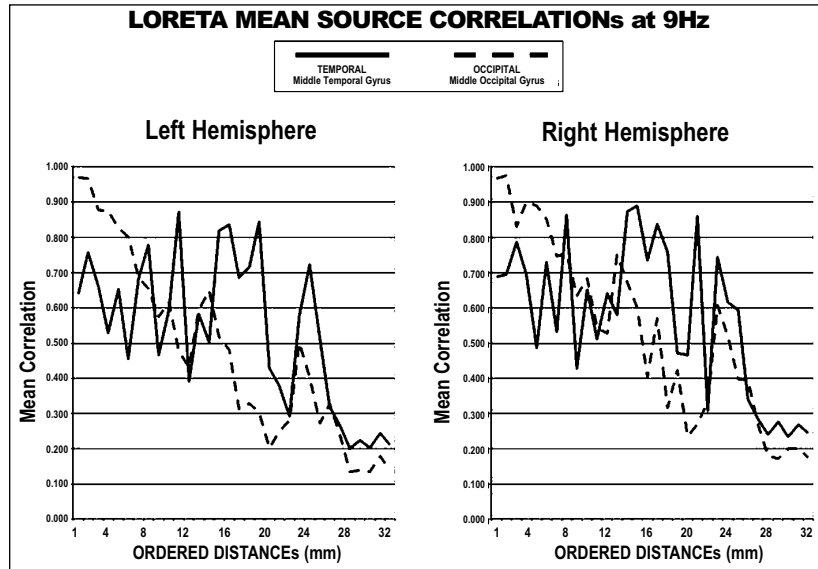
tive) are colored orange to red. T-test differences where the right hemisphere source correlations were greater than the homologous left hemisphere source correlations (negative) are colored blue to purple. In contrast to the superior frontal gyrus, the right middle occipital gyrus source correlations are significantly greater than left hemisphere source correlations (i.e., blue and purple colors) especially at middle to long distances (43 mm to 94 mm) especially in the 1 to 15 Hz range. In general, the right hemisphere occipital source correlations are greater than the left homologous left hemisphere occipital regions.

Hemispheric differences in regions of interest independent of frequency

In order to evaluate and summarize the strength of the hemispheric differences in source correlations the number of statistically significant t-tests (P < .05) were tabulated for the four lobules (frontal, temporal, parietal and occipital) by combining regions of interest that are contained within a given lobule. Figure 7 shows the tabulation of statistically significant t-tests in lobules independent of frequency. The ROIs that comprise a given lobule are on the x-axis and the number of statistically significant t-tests (P < .05) are on the y-axis. T-tests where the left hemisphere source correlations were significantly greater than the homologous right hemisphere are represented by the open bars and t-tests where the right hemisphere source correlations were significantly greater than the homologous left hemisphere are represented by the black bars. The total number of t-tests equals the number of ROIs or 32 times the 40 frequencies = 1,280. One would expect 64 statistically significant t-tests by chance alone at P < .05. It can be seen that only the frontal lobules

exhibited greater left than right hemisphere source correlations, with the exception of the pre-central gyrus which exhibited greater right hemisphere source correlations than left hemisphere. All other lobules (temporal, parietal and occipital) exhibited greater right hemisphere source correlations than the left hemisphere. The greatest right hemisphere asymmetry in the temporal lobule was in the inferior temporal gyrus (ITG), the greatest right hemisphere asymmetry in the parietal lobule was in the superior parietal lobule (SPL), and the greatest right hemisphere asymmetry in the occipital lobule was in the middle occipital gyrus (MOG).

Hemispheric differences in frequency independent of regions of interest

Figure 8 shows the total number of statistically significant t-tests (P < .05) from 1 to 40 Hz for all ROIs combined. The total number of t-tests in this analysis equals the number of ROIs or 33 times the remaining regions that are correlated with each region = 32 and 33 x 32 = 1,056. One would expect 53 statistically significant t-tests by chance alone at P < .05. The dashed lines represent right hemisphere greater than left hemisphere significant differences and the solid lines represent left hemisphere greater than right. It can be seen that the alpha frequency band (8 to 12 Hz) exhibited the greatest right > left hemispheric differences. In contrast, the left hemisphere exhibited greater source correlations than the homologous right hemisphere in the higher frequency range, 37 - 40 Hz.

Figure 9 shows a break down of the overall summary of statistically significant t-tests as a function of lobule and frequency. The total number of t-tests in this analysis is different for each lobule, because each lobule has a different
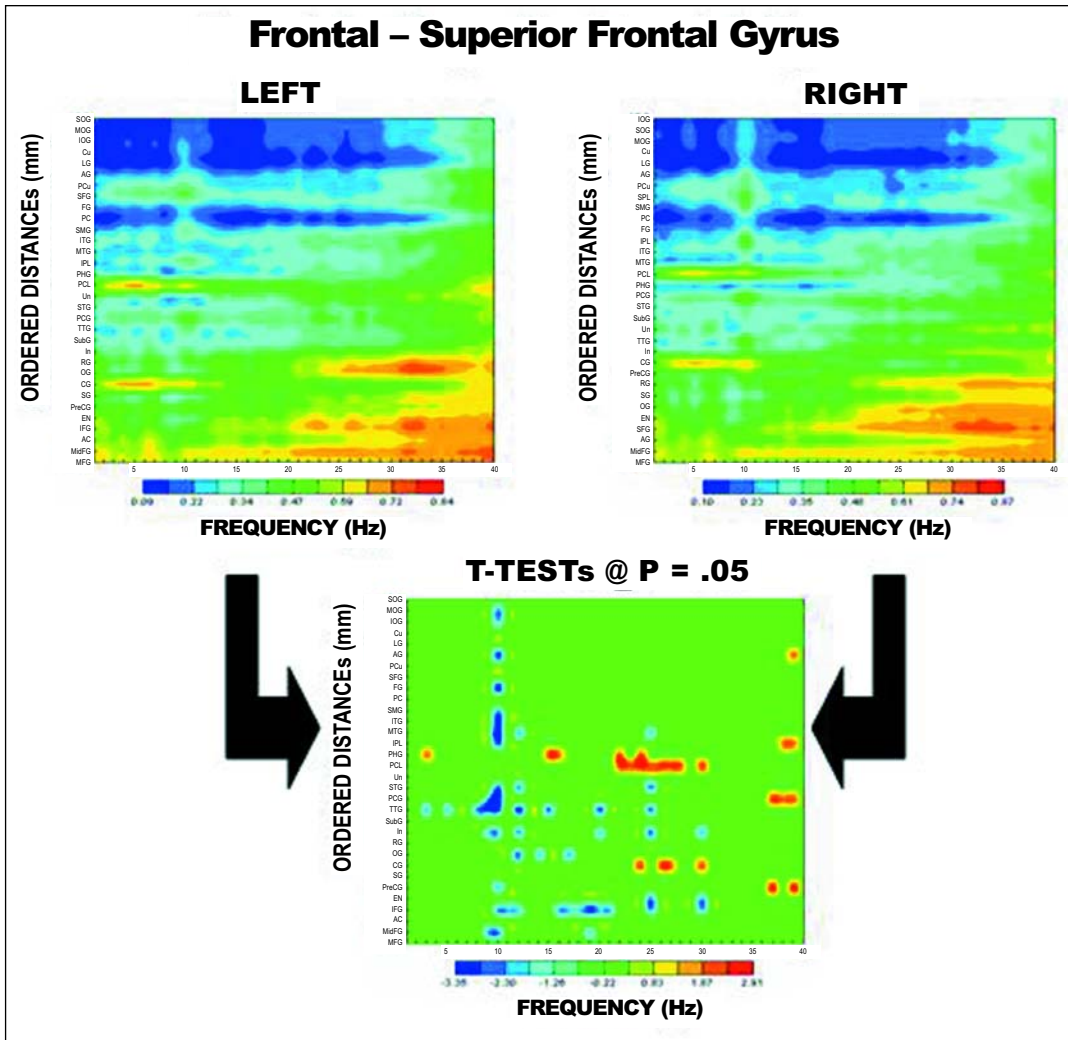
Figure 5.
Top left are mean source correlations from the left intra-hemisphere superior frontal gyrus and the top right are the mean source correlations from the homologous right superior frontal gyrus. The y-axis are ROIs that are ordered as a function of distance from the superior frontal gyrus. The x-axis is frequency from 1 to 40 Hz and the z-axis is the magnitude of correlation as shown by the color bar. The middle contour map are t-test values between the left and right hemisphere superior frontal gyrus. The z-axis is the magnitude of the t-values as shown in the color bar. See Table 1 for the listing of ROIs.

number of ROIs. For the frontal lobule the total number of t-tests = 11 x 32 = 352 (18 by chance alone), parietal lobes = 9 x 32 = 288 (14 by chance alone), temporal lobes = 8 x 32 = 256 (13 by chance alone) and the occipital lobes = 5 x 32 = 160 (8 by chance alone). It can be seen that there is a maximum in the alpha frequency range (8 - 12 Hz) in all lobules and the direction of differences in the alpha band is always right greater than left. With the exception of the occipital lobule, the left hemisphere source correlations are greater than the homologous right hemisphere in the higher frequency range (37 - 40 Hz).

DISCUSSION

The results of this study demonstrated spatial-temporal patterns of correlation between EEG current sources within specific regions of the cortex. Contrary to a monotonic point-spread function, spatial and temporal patterns were present in all subjects as well as in averages from all ROIs. Spatial heterogeneity and anatomical specificity were consistently demonstrated by spatial rhythms of correlations at specific frequencies that varied according to the location of the reference region of interest. Therefore, all three uniform null hypotheses discussed in the Introduction can be rejected.
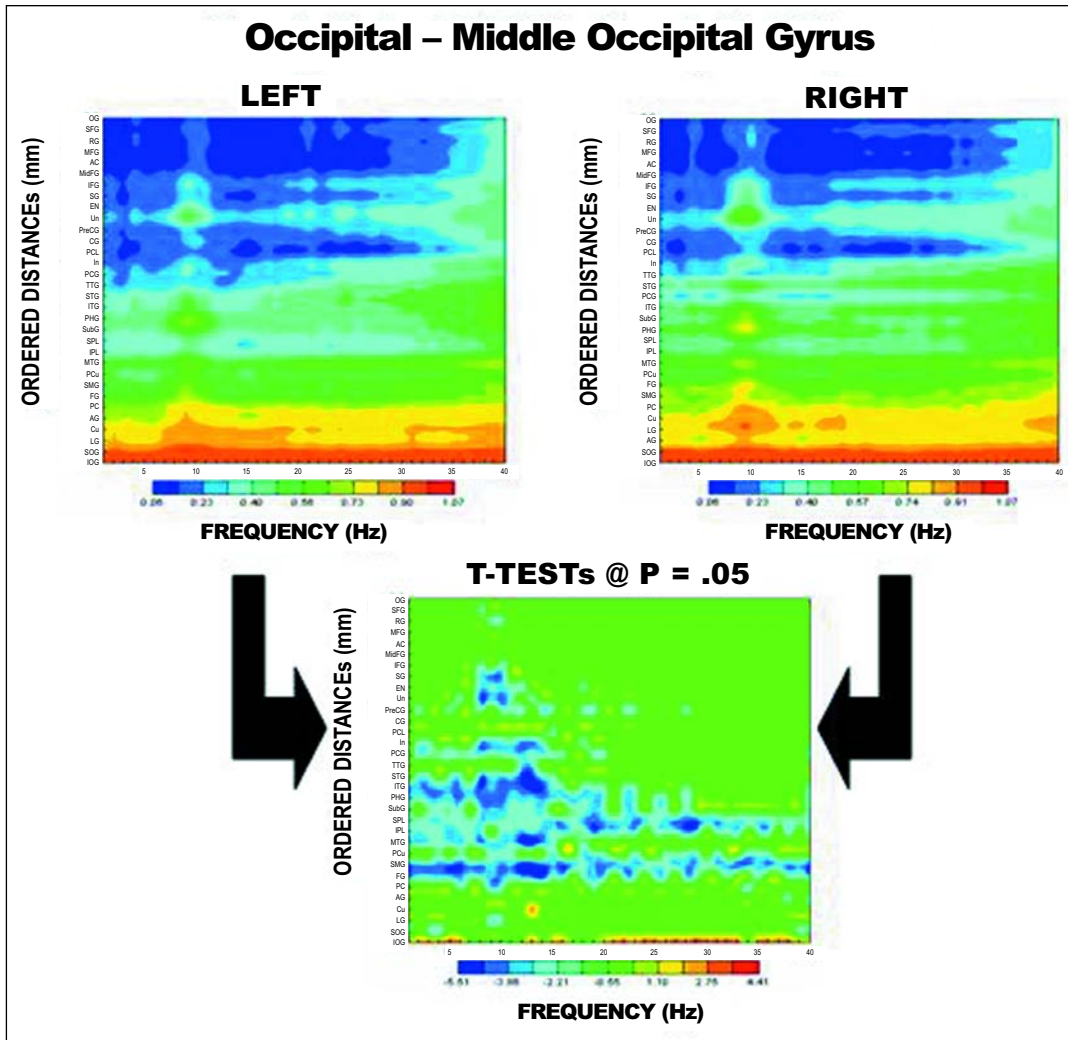
Figure 6.
Top left are mean source correlations from the left hemisphere middle occipital gyrus and the top right are the mean source correlations from the right hemisphere middle occipital gyrus. The y-axis are ROIs that are ordered as a function of distance from the middle occipital gyrus. The x-axis is frequency from 1 to 40 Hz and the z-axis is the magnitude of correlation as shown by the color bar. The middle contour map are t-test values between the left and right hemisphere middle occipital gyrus. The z-axis is the magnitude of the t-values as shown in the color bar.

The finding of spatio-temporal heterogeneity was observed in all of the individual subjects (Figures 2, 3, 4, 5). The occipital lobes exhibited maximum correlation at short distances (10 mm to approx. 20 mm) while the frontal lobes exhibited maximum correlations at longer distances (50 mm to 105 mm), and the temporal and parietal lobes exhibited a mixture of short and long distance correlations. All regions of interest exhibited rhythmic increases and decreases in spatial-temporal correlation as a function of distance. In this study the temporal dimension is the correlation of current source density from successive 2 second samples of alert eyes-closed

EEG over an interval of time that varied between 58.6 to 120 seconds. Similar heterogeneities were also observed in unpublished analyses of eyes-open EEG data. Importantly, each ROI exhibited maximum correlations to other ROIs at different frequencies. In general, short distance correlations tended to be frequency independent while long distance correlations were more frequency specific. Further, longer inter-region distances were most strongly associated with higher frequencies (20 - 40 Hz). These findings are similar to those reported by Shen et al[7] using EEG coherence recorded from arrays of subdural electrodes. For example, Shen et al[7]
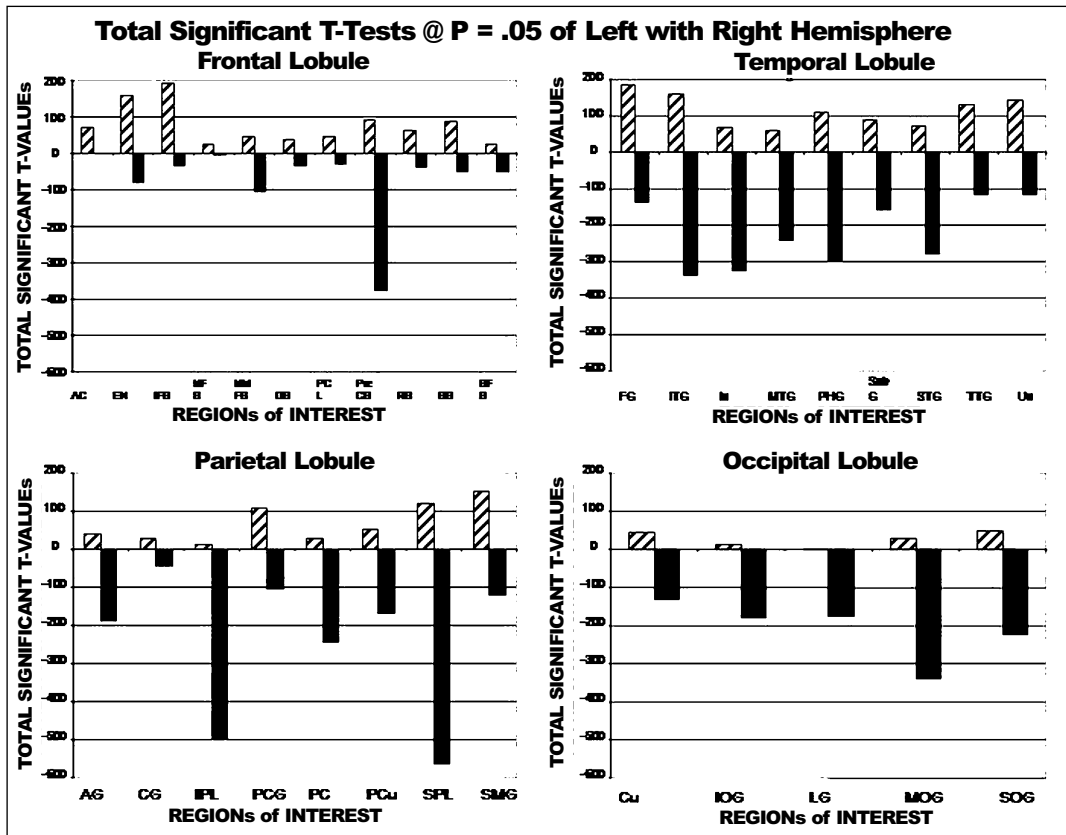
Figure 7.
Total number of statistically significant t-tests (P < .05) between the left and right hemisphere source correlations for different ROIs. Number of negative t-values is Right hemisphere > Left hemisphere and number of positive t-values is Left hemisphere > Right hemisphere. Top left are the number of statistically significant source correlations in different ROIs between the left and right frontal lobules. Top right are the number of statistically significant source correlations in different ROIs between the left and right temporal lobules. Bottom left are the number of statistically significant source correlations in different ROIs between the left and right parietal lobule and the bottom right are the number of statistically significant source correlations in different ROIs between the left and right occipital lobules. Oblique columns are positive t-values in which the left hemisphere source correlations are greater than the homologous right hemisphere source correlations. Black columns are negative t-values in which the right hemisphere source correlations are greater than the homologous left hemisphere source correlations.

reported that lower frequencies were associated with short interelectrode distances, and that specific locations in the subdural grid of electrodes were associated with distant locations at specific frequencies.

Limitations of this study

As mentioned in the Introduction a general limitation of all LORETA studies is the use of a "Low Resolution" point spread function by the Laplacian operator when using 19 scalp electrodes (Pascual-Marqui.[12] A point-spread means that the spatial correlation is approximately unity between nearby voxels and decreases as a monotonic function of distance. The design of the present study minimized the effects of the point spread of current density estimates by clustering hundreds of nearby voxels into "Regions of Interest" This strategy appears effective since if the point

spread function were dominant then there should always be high correlations near to the reference ROI, which is contrary to the finding that only the occipital regions and not frontal regions exhibited short distance spatial correlations. In addition, the point spread function can not explain the presence of spatial frequencies and maxima at long distances (see Figures 2-8), because the correlations in this study are spatial covariances of the time series of current densities and the point-spread function is constant as a function of time. Another limitation is the use of the Pearson product correlation for the time series of magnitudes over time rather than the computation of coherence and phase. Coherence and phase are more fundamental to the measures of oscillator coupling than is a spatial-temporal Pearson product correlation coefficient of magni-
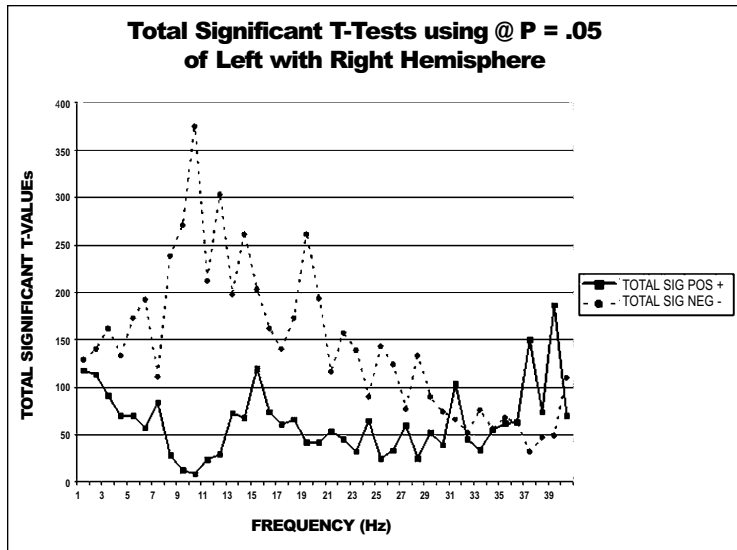
Figure 8.
Total number of statistically significant t-tests between the left and right hemisphere source correlations as a function of frequency. The solid line is positive t-values in which the left hemisphere source correlations are greater than the homologous right hemisphere source correlations. The dotted line is the number of negative t-values in which the right hemisphere source correlations are greater than the homologous left hemisphere source correlations. The y-axis is the number of statistically significant t-values (P < .05) and the x-axis is frequency from 1 to 40 Hz.

tudes. Nevertheless, the Pearson product correlation coefficient is a valid measure especially when the intent is to estimate the covariance of magnitudes over a relative long interval of time. Coherence and phase are valuable measures and we plan to implement these measures in the future. A passive condition such as eyes-closed resting is another possible limitation because active task dynamics may be related to the strength and modulation of coupling.

Source correlations and cortico-cortical connectivity

There were several consistent and distinct features in the source correlations observed in this study. One distinct feature was that all source correlations showed rhythmic increases and decreases in the strength of correlation as a function of distance from a ROI (Figures 2-9). Another distinct feature was that the occipital lobes showed the strongest correlations at short distances (2 mm to 20 mm) while the frontal lobes exhibited longer peak-to-peak correlation distances than the occipital lobes. These findings are consistent with the higher packing density of occipital lobes compared to the frontal lobes[17,18] and with distance estimates of cortico-cortical 'U' shaped fiber bundles that connect cortical gyri and sulci. The findings are consistent with a 'U' shaped cortico-cortical connection system in the cerebral cortex.

This model assumes that the short distance horizontal bands, e.g., 1 cm to 3 cm observed in Figures 2 and 3 are influenced by the 'U' shaped cortico-cortical fiber systems studied by Schulz and Braitenberg[4] and Braitenberg[3]. For example, Schulz and Braitenberg[4] showed that there are three categories of cortico-cortical connections in the human brain: 1- intra-cortical connections which represent the majority of cortical connections and are on the order of 1 mm to approximately 5 mm and involve collateral axonal connections that do not enter the cerebral white matter; 2-'U' shaped myelinated fibers representing the majority of the cerebral white matter that connect cortical gyri and sulci and are on the order of 3 mm to 3 cm and, 3- deeply located long distance fiber systems referred to as fasciculi with connections from approximately 3 to 15 cm that represent approximately 4% of the cerebral white matter.

The intra-cortical fiber system is too short at 1 to 3 mm for the 19 lead or even 512 lead EEG to resolve at the scalp surface (see system 'A' in Figure 10). Nonetheless, the effects of the intra-cortical system on the amplitude of the EEG are very strong, because fiber bundles carry action potentials that terminate that produce excitatory post-synaptic potentials and thereby synchronize activation of small to large domains of cells which produce currents that are recorded electrically as the surface EEG. The LORETA inverse solution of the scalp-recorded EEG uses a Laplacian operator to emphasize the contribution of distributed and synchronous current source activation, which must as a matter of physics be influenced by neuronal packing density, e.g., resulting in high occipital short distance correlations.

The contribution of the 'U' shaped fiber system is seen best in the horizontal bands of high correlation at 30 mm to approximately 60 mm such as in Figures 2 and 3. Support for a cortico-cortical 'U' shaped fiber hypothesis in the present study is the finding of peak-to-peak correlation distances that ranged from approximately 20 mm to 40 mm (see Figures 2-8), which is in the range of distances known to exist for the 'U' shaped fiber systems of the human brain. The 'U' shaped cortico-cortical fiber hypothesis is also supported by the finding of a much smaller contribution by the long distance connection system that was also observed, especially in frontal and occipital ROIs, and was on the order of 8 to 12 cm, which is consistent with Schulz and Braitenberg[4] (see Figures 2 and 3). Figure 10 is an illustra-
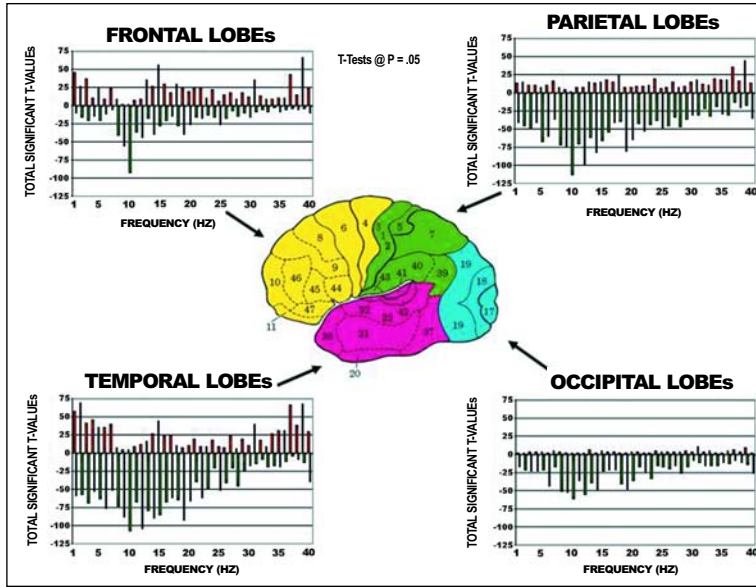
Figure 9.
Total number of statistically significant t-values (P < .05) between the left and right hemisphere source correlations in four different lobules at different frequencies. Negative t-values means the right hemisphere correlations > the left hemisphere and positive t-values mean the left hemisphere correlations > right hemisphere. The top left is from the frontal lobes, the top right is from the parietal lobes, the bottom left is from the temporal lobes and the bottom right is from the occipital lobes. The y-axis is the number of statistically significant t-values (P < .05) and the x-axis is frequency from 1 to 40 Hz.
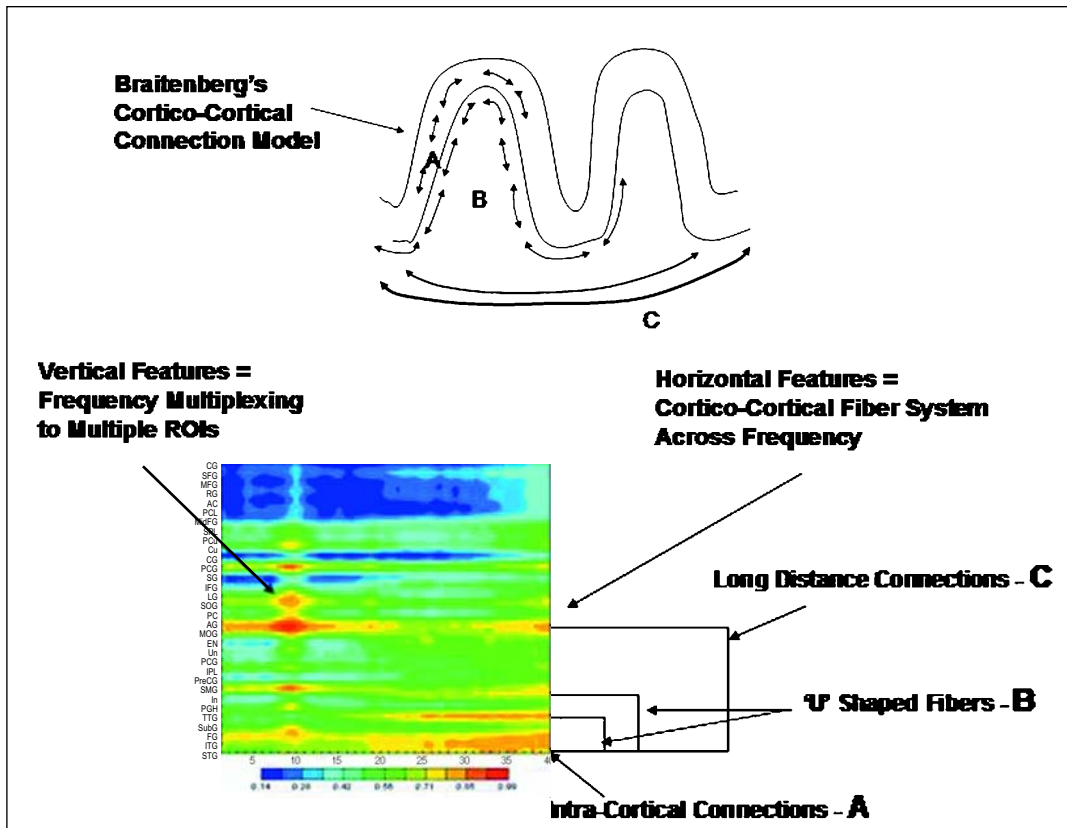

Figure 10.
Diagrammatic illustration of a cortico-cortical connection model. Top is the organization of intra-cortical connections according to Schulz and Braitenberg.[4] A = gray matter intra-cortical connections, B = 'U' shaped white matter connections and C = long distance white matter connections. Bottom is an exemplar contour map of source correlations in which the horizontal bands of increasing and decreasing source correlations correspond to the different cortico-cortical connection systems as described in the top of the figure.

tion of a cortico-cortical connection model based on Shultz and Braitenberg[3] to explain the source correlation findings in this study. Additional support for a cortico-cortical hypothesis is the finding of no difference in left and right hemisphere peak-to-peak spatial oscillations of source correlations, which is consistent with studies by Schulz and Braitenberg[4] who failed to find significant hemispheric differences in the length of the long distance and 'U' shaped fiber connections.

The lack of difference in the distances between inter-peak correlations in left and right hemispheres in the present study indicates that the intrinsic fiber connection system is an invariant and stable variable, which is similar for the left and right hemispheres. Significantly, while inter-peak differences are the same between left and right hemispheres the magnitude of source correlations is generally greater in the right hemisphere than in the left hemisphere (see Figures 7 and 8). This indicates that the number or strength of intra-hemispheric connections, i.e., coupling magnitude, is generally greater in the right hemisphere than in the left hemisphere. The exception is in the frontal lobes and higher EEG frequencies.

Evidence of cortico-cortical multiplexing

Another distinct feature of the correlation contour maps was the presence of vertical bands of high or low correlation at specific frequencies (see Figures 2-8). The alpha frequency band was often prominent in occipital and parietal ROIs and less prominent in temporal and frontal ROIs. The frontal and temporal ROIs often showed maximal correlations at higher frequencies (e.g., 30-40 Hz), but each ROI showed maximal correlations at specific frequencies with single or a particular group of ROIs (see Figures. 2, 3, 4, 5, 7 and 11). These findings are similar to those reported by Shen et al[7] using coherence of EEG recorded from subdural electrodes in which specific locations in the electrode grid exhibited high coherence to another location but at a specific frequency. In fact, the authors reported that each subdural electrode exhibited a unique spatial-frequency relationship to all other locations in the grid of electrodes; they presented a type of multiplexing model in which each domain of neurons communicated with all other domains but at specific frequencies. The present findings are consistent with the Shen et al[7] "spatial-spectral signature of cortical synchrony" model of cortico-cortical coupling. According to this model, each ROI is connected to all other ROIs but a given region communicates at specific frequencies.

As presented previously, the individual subject findings and the statistically significant covariance between distant locations of the brain over time at a specific frequency is evidence of a stable resonance. If we assume that the connections between two ensembles are stable and mediated by axonal fibers which conduct all frequencies, then resonance at a specific frequency occurs when phase locking between the two connected neuronal ensembles is opti-

mal. A model of the spatial frequency of current density variation between two distant locations at a given temporal frequency is consistent with a stable 'U' shaped fiber system and long distance fasciculi in which all frequencies are conducted with the number of synapses and dendritic location of synapses and thalamo-cortical synchronizing mechanisms governing the spatial covariances of a given ROI.

Hemispheric differences in cortico-cortical connectivity

The results of this study showed that, in general, the right hemisphere exhibited higher intra-hemispheric source correlations than the left hemisphere, with the exception of the frontal lobes. Right greater than left was especially the case for parietal and occipital lobules. The frontal and temporal lobules showed higher left intra-hemispheric source correlations than in the homologous right hemisphere between 1 to 5 Hz, 15 Hz and 35-40 Hz. The right intra-hemispheric correlations were significantly greater than the homologous left hemisphere at 10 Hz in all lobules. The occipital lobes were unique in that there were greater right intra-hemispheric significant correlations than the homologous left hemisphere at all frequencies.

The largest hemispheric asymmetries were in the superior parietal lobule and the inferior parietal lobule with greater right intra-hemispheric source correlations than in the homologous left hemisphere (see Figure 9). A rank ordering of the most statistically significant intra-hemispheric asymmetries of the right greater than left hemisphere is: superior parietal gyrus > inferior parietal gyrus > pre-central gyrus > middle occipital gyrus > inferior temporal gyrus > insula.

The finding of greater right intra-hemispheric source correlations than in the left hemisphere is consistent with coherence studies of the surface EEG in which there is greater right hemispheric coherence than in the left hemisphere in both longitudinal and cross-sectional studies.[5,19,20] The LORETA current density findings in the present study and the surface EEG findings are also consistent with MRI studies showing a higher white matter to gray matter ratio in the right hemisphere in comparison to the left.[21] For example, the left hemisphere is more highly fissured than the right[22] with a higher density of cells in the left than in the right hemisphere,[23] as well as a longer planum temporale and longer sylvian fissure in the left hemisphere.[24,25] The findings from these studies and the present study when taken as a whole indicate that the organization of the left hemisphere favors processing or transfer within cortical regions, whereas the right hemisphere is more specialized for the processing or integration of information across regions. Given these considerations, the findings in the present study are consistent with functional differences between the human left and right hemispheres in which the left hemisphere is involved in analytical and sequential processing in contrast to the right hemisphere which is more involved in synthesis and integration and relational functions.[26] More specifically, the left hemisphere has been

shown to be strongly involved in analytical and sequential processing, which would presumably require a high degree of local differentiation, whereas the right hemisphere is more involved in synthesis and relational functions which would require more intrahemispheric fibers to coordinate and relate the outputs of the distributed local processors. The finding of greater spatial correlations in the right hemisphere compared to the left hemisphere is consistent with these functional models of hemispheric specialization.

The use of source correlation and source coherence has been shown to be a useful method for exploring corti-

co-cortical connectivity as well as the temporal-spatial dynamics involved in cognition and clinical applications.[8-11] The present study further supports the use of source correlation and source coherence as a reliable and clinically useful digital signal processing tool. Finally, interhemispheric correlations were not explored in the present study. Shultz and Braitenberg[4] estimate that only approximately 3% of the cerebral white matter involves direct hemispheric connections such as through the corpus callosum, and the application of source correlations to interhemispheric relationships will be the subject of a future study.

REFERENCES

1. Nunez P. Electrical Fields of the Brain. New York: Oxford University Press; 1981.

2. Nunez P. Neocortical Dynamics and Human EEG Rhythms. New York: Oxford University Press; 1994.

3. Braitenberg, V. Cortical architectonics: general and areal. In: Brazier MAB, Petsche H, (eds). Architectonics of the Cerebral Cortex. New York: Raven Press; 1978: 443-465.

4. Schulz A, Braintenberg V. The human cortical white matter: quantitative aspects of cortico-cortical long-range connectivity. In: Schultz A, Miller R, (eds). Cortical Areas: Unity and Diversity. Conceptual Advances in Brain Research, London, 2002: 377-386.

5. Thatcher RW, Krause P, Hrybyk M. Corticocortical association fibers and EEG coherence: a two compartmental model. Electroencephalogr Clin Neurophysiol 1986; 64: 123-143.

6. Thatcher RW, Biver C, McAlaster R, Salazar AM. Biophysical linkage between MRI and EEG coherence in traumatic brain injury. NeuroImage 1998; 8(4): 307-326.

7 Shen B, Nadkarni M, Zappulla RA. Spatial-spectral signature of human cortical synchrony. EEG Clin Neurophysiol 1999; 110(1): 115-125.

8. Thatcher R, Wang B, Toro C, Hallett M. Human neural network dynamics using multimodal registration of EEG, PET and MRI. In: Thatcher R, Hallett M, Zeffiro T, John E, Huerta M, (eds). Functional Neuroimaging: Technical Foundations. New York: Academic Press; 1994.

9. Thatcher RW. Tomographic electroencephalography/magnetoecephalography: dynaics of human neural network switching. J Neuroimag 1995; 5: 35-45.

10. Hoechstetter K, Bornfleth H, Weckesser D, Ille N, Berg P, Scherg M. BESA source coherence: a new method to study cortical oscillatory coupling. Brain Topogr 2004; 16: 233-238.

11. Pascual-Marqui RD, Koukkou M, Lehmann D, Kochi K. Functional localization and functional connectivity with LORETA comparison of normal controls and first episode drug naïve schizophrenics. J Neurotherapy 2001; 4(4): 35-37.

12. Pascual-Marqui RD. Review of methods for solving the EEG inverse problem. Int J Bioelectromagnetism 1999; 1:75-86.

13. Gomez J, Thatcher RW. Frequency domain equivalence between potentials and currents using LORETA. Int J Neurosci 2001; 107: 161-171.

14. Frei E, Gamma A, Pascual-Marqui RD, Lrhmsnn D, Hell D, Vollenweider FX. Localization of MDMA-induced brain activity in healthy volunteers using low resolution electromagnetic tomography (LORETA). Human Brain Map 2001; 14: 152-165.

15. Pascual-Marqui RD. Free software and documentation from the Key Institute that was downloaded from http://www.unizh.ch/keyinst/NewLORETA/Software/Software.htm. June, 2003.

16. Lancaster JL, Woldorff MG, Parsons LM, Liotti M, Freitas CS, Rainey L, et al. Automatice Talairach atlas labels for functional brain mapping. Human Brain Map 2000; 10: 120-131

17. Blinkov SM, Glezer I. The Human Brain in Figures and Tables: A Quantitative Handbook. New York: Basic Books, Plenum Press; 1968.

18. Carpenter MB, Sutin J. Human Neuroanatomy. 8th ed. Baltimore, Maryland: Williams and Wilkins; 1983.

19. Tucker DM, Dawson SL, Roth DL, Penland JG. Regional changes in EEG power and coherence during cognition: intensive study of two individuals. Behav Neurosci 1985; 99(3):564-77.

20. Tucker DM, Roth DL, Blair TB. Functional connections among cortical regions: Topography of EEG coherence. Electroenceph Clin Neurophysiol 1986; 63: 242-250.

21. Gur RC, Packer IK, Hungerbuhler JP, Reivich M, Obrist WD, Amarnek WS, Sacheim HA. Differences in the distribution of gray and white matter in human cerebral hemispheres. Science 1980; 207: 1226-1228.

22. Connelly CJ. External Morphology of the Primate Brain. Springfield, IL: Charles C Thomas; 1950.

23. Galaburda AM, LeMay M, Kemper TL, Geschwind N. Right-left asymmetries in the brain. Science 1978; 199: 852-856.

24. Geschwind N, Levitski W. Human brain: left-right asymmetries in temporal speech region. Science 1968; 161: 186-187.

25. Chi HJG, Dooling ES, Giles FH. Gyral development of the human brain. Ann Neurol 1977; 1: 86-94.

26. Kinsbourne M. Mechanisms of hemisphere interaction in man. In: Kinsbourne M, Smith L, (eds). Hemispheric Disconnection and Cerebral Function. Thomas, Springfield, IL: Charles C Thomas; 1974: 71-86.